



THE UNIVERSITY *of* EDINBURGH

Edinburgh Research Explorer

Adaptive Switching Detection Algorithm for Iterative-MIMO systems to Enable Power Savings

Citation for published version:

Tadza, NZBM, Laurenson, D & Thompson, J 2014, 'Adaptive Switching Detection Algorithm for Iterative-MIMO systems to Enable Power Savings' Radio Science., 10.1002/2013RS005323

Digital Object Identifier (DOI):

[10.1002/2013RS005323](https://doi.org/10.1002/2013RS005323)

Link:

[Link to publication record in Edinburgh Research Explorer](#)

Document Version:

Author final version (often known as postprint)

Published In:

Radio Science

General rights

Copyright for the publications made accessible via the Edinburgh Research Explorer is retained by the author(s) and / or other copyright owners and it is a condition of accessing these publications that users recognise and abide by the legal requirements associated with these rights.

Take down policy

The University of Edinburgh has made every reasonable effort to ensure that Edinburgh Research Explorer content complies with UK legislation. If you believe that the public display of this file breaches copyright please contact openaccess@ed.ac.uk providing details, and we will remove access to the work immediately and investigate your claim.



¹ **Adaptive Switching Detection Algorithm for**
² **Iterative-MIMO systems to Enable Power**
³ **Savings**

N Tadza,¹ D Laurenson,¹ and J S Thompson¹

Corresponding author: N Tadza, Institute for Digital Communications, School of Engineering, University of Edinburgh, EH9 3JL, Edinburgh, UK. (n.tadza@ed.ac.uk)

¹Institute for Digital Communications,
School of Engineering, The University of
Edinburgh, EH9 3JL, Edinburgh, UK.

4 This paper attempts to tackle one of the challenges faced in soft input soft
5 output Multiple Input Multiple Output (MIMO) detection systems, which
6 is to achieve optimal error rate performance with minimal power consump-
7 tion. This is realized by proposing a new algorithm design that comprises
8 multiple thresholds within the detector that, in real time, specify the receiver
9 behavior according to the current channel in both slow and fast fading con-
10 ditions, giving it adaptivity. This adaptivity enables energy savings within
11 the system since the receiver chooses whether to accept or to reject the trans-
12 mission, according to the success rate of detecting thresholds. The thresh-
13 olds are calculated using the mutual information of the instantaneous chan-
14 nel conditions between the transmitting and receiving antennas of iterative-
15 MIMO systems. In addition, the power saving technique, Dynamic Voltage
16 and Frequency Scaling, helps to reduce the circuit power demands of the adap-
17 tive algorithm. This adaptivity has the potential to save up to 30% of the
18 total energy when it is implemented on Xilinx®Virtex-5 simulation hard-
19 ware. Results indicate the benefits of having this ‘intelligence’ in the adap-
20 tive algorithm due to the promising performance-complexity trade-off pa-
21 rameters in both software and hardware co-design simulation.

1. Introduction

22 The ability to increase throughput without requiring more computational power
23 has always been a topic of interest amongst the wireless communication research com-
24 munity. Multiple Input Multiple Output (MIMO) promises high throughput without
25 additional transmit power [*Goldsmith et al., 2007*], however, minimizing the receiver's
26 power, which is often limited, is still under intensive study. Current base stations,
27 proliferations of femtocells and/or wireless access points also need to exercise being
28 'green'. The energy source is often shared amongst millions of devices. There are
29 substantial potential of power savings to be gained in these small mains powered de-
30 vices. In this paper, a field programmable gate array (FPGA) is used as a platform to
31 show the inner workings of the adaptive algorithm. It is chosen due to its robustness,
32 its reprogrammable capabilities and its potential for further energy savings by paral-
33 lelization. The results obtained can be translated onto any hardware platform such
34 as an application-specific integrated circuit (ASIC), which is more common in mobile
35 devices. Fundamentally, a soft-MIMO receiver is divided into two parts, the MIMO
36 detector and the soft decoder working together to achieve the best performance. The
37 received data is processed through the detector before being passed into the decoder.
38 Most publications focus on saving power using the signal-to-noise ratio (SNR) [Wu,
39 2011], channel matrix condition number [Matthaiou et al., 2008] or reducing the
40 number of turbo decoding iterations [Zhang et al., 2009] for the receiver. Condition
41 numbers of the channel matrix would only take into account the input and output
42 matrix of the transmitter and the receiver. This is not sufficient as a switching metric

43 since it disregards the noise level. SNR on the other hand, does not compute the re-
44 lationship between the antennas in a MIMO system. If the channel is deemed good,
45 due to high SNR values; strongly correlated antennas would not make for a good
46 transmission condition. This is because the correlated system provides insufficient
47 diversity in the MIMO system. Therefore, mutual information (MI) is implemented
48 due to its consideration of the diversity of a MIMO system i.e. the transmitters and
49 the receivers as well as the noise level. This gives a maximum amount of information
50 regarding a channel with minimal complexity in comparison to using either condition
51 number or SNR alone. This paper therefore, shifts the attention to the detector using
52 MI as the threshold control; in hope to gain energy savings earlier on the processing
53 stages i.e. by avoiding both detection and decoding processing. This iterative-MIMO
54 scheme, which combines a spatial multiplexing MIMO detector and an outer forward
55 error correction soft decoder with an interleaver in-between [*Ariyavisitakul, 2000*]
56 [*Sellathurai and Haykin, 2002*], dubbed Bit-Interleaved Coded Modulation (BICM),
57 [*Hochwald and ten Brink, 2003*], has very high computational complexity as the re-
58 ceiver detects and decodes symbols by searching through possible transmit symbols.
59 Moreover, this is done iteratively in soft-MIMO detection systems by the decoder.

60 This paper focuses on saving energy consumption in the MIMO detector, where it
61 predicts symbols transmitted by each antenna by examining the channel noise and
62 constellation modulation scheme. It should be noted that, though out of scope of the
63 paper, after the process of detecting, the symbols are passed to the outer decoder
64 before a hard decision can be made.

65 There are many types of different detection algorithms available, which can be
66 generalized into “Nulling and Cancelling” methods, such as the Zero Forcing (ZF)
67 [*Winters et al.*, 1994] and the Minimum Mean Square Error Estimation (MMSE)
68 [*Li et al.*, 2006] techniques as well as the “Tree Search” algorithms, for instance,
69 the Maximum Likelihood (ML), Sphere Decoding (SD) [*Fincke and Pohst*, 1985],
70 and the Fixed Sphere Decoding (FSD) [*Barbero and Thompson*, 2008] routines. For
71 simple detectors, ZF and MMSE provide low complexity, however, they give poor
72 performance in terms of bit-error-rate (BER). Linear detection methods, combined
73 with nulling and cancelling, seem to give a better BER whilst maintaining the low
74 complexity. This is why the combination of V-BLAST and ZF is chosen. On the
75 other hand, for close to ML performance, tree search algorithms such as FSD, lay-
76 ered orthogonal lattice detector (LORD), smart ordered candidate adding algorithm
77 (SOCA) and K-Best result in high complexity in order to meet the performance cri-
78 teria. This drains a lot of power in order to decode data packets, which is particularly
79 wasteful in good channel conditions. In poor channel conditions, FSD has been cho-
80 sen as a detection method as it is independent of the search radius, meaning, the
81 complexity is fixed and minimal in comparison to other tree search algorithms. The
82 novelty of this paper lies in the fact that the algorithm switches between high and
83 low complexity detectors to give a bigger gain in energy savings. Ultimately, using
84 different detectors would only slightly alter the thresholds that need to be imple-
85 mented, confirming that MI is adaptive to any system for determining the threshold
86 for switching.

87 The computational power required to implement tree search MIMO detection ev-
88 ery time a symbol is transmitted is unnecessary in some channel conditions. As
89 each detection algorithm has a different performance and complexity, choosing be-
90 tween them depends on the system's unique requirements. To construct an adaptive
91 implementation that could fit on available hardware in the market, this study com-
92 bines two detection algorithms. The Fixed Sphere Decoding (FSD) and the Vertical
93 Bell Laboratories Layered Space Time/Zero Forcing (V-BLAST/ZF) techniques are
94 incorporated into an adaptive approach that has the ability to selectively operate ac-
95 cording to the received signal conditions. These two detection algorithms are chosen
96 due to their fixed data throughput, potential for hardware parallel implementation
97 and low complexity.

98 The proposed adaptive algorithm therefore prevents the receiver from performing
99 extensive computation under very low or very high SNR conditions, which ultimately
100 yields significant savings in energy. The algorithm utilizes multiple thresholds to
101 intelligently switch MIMO detection schemes according to the current environment.
102 This 'intelligence' is the key to efficient energy utilization in the receiver. The results
103 of this work will be presented in terms of overall energy savings from both software
104 and hardware standpoints.

1.1. Contributions

105 The main contributions of this paper are summarized as follows:

- 106 • An adaptive switching algorithm that adapts to real time channel conditions by
107 selecting to minimize the power consumption of iterative-MIMO detection systems is

108 proposed. This is realized in the form of a threshold control unit, which selects the
 109 minimum complexity detector capable of meeting the desired BER performance.

110 • The adaptive algorithm shows promising BER performance on a par with the
 111 current available detection schemes with lower computational complexity.

112 • An evaluation of the new design in a Xilinx® Virtex-5 FPGA shows convincing
 113 dynamic and static power savings compared to baseline detectors.

2. Background

2.1. System Model

114 Consider an iterative-MIMO system comprising M transmit antennas and N re-
 115 ceive antennas based on BCIM, transmitting frames of K_u bits as shown in Figure
 116 1. At the transmitter, the K_u bits are encoded using an iterative encoding method
 117 such as convolutional or turbo coding [*Hagenauer et al.*, 1996] of rate R_c , where
 118 $K_u = K_e \cdot R_c$. The K_e coded bits are then interleaved giving K_a bits, which are
 119 mapped into independent Quadrature Amplitude Modulation (QAM) constellations,
 120 \mathcal{O} , of P points, forming a sequence of $K_s = K_e / \log_2 P$ symbols. The symbols are
 121 separated into M substreams blocks of $M \cdot K_{ch}$ symbols are transmitted in each
 122 channel realization, K_{ch} . These are transmitted over Rayleigh fading channels. In
 123 other words, a frame of K_e coded bits requires a transmission of $K_s / (M \cdot K_{ch})$ blocks
 124 of data. Consequently, the received symbols, indexed by a sample time, k , can be
 written as

$$125 \quad \mathbf{r}[k] = \mathbf{H}[k]\mathbf{s}[k] + \mathbf{n}[k] \quad (1)$$

126 where the channel matrix $\mathbf{H} \in \mathbb{C}^{M \times N}$ is assumed to be perfectly known at the
 127 receiver with independent elements $h_{i,j} \sim \mathcal{CN}(0, 1)$, for $1 \leq i \leq M$ and $1 \leq j \leq N$
 128 representing a block Rayleigh fading propagation environment, $\mathbf{s} = (s_1, s_2, \dots, s_M)^T$
 129 is the transpose vector of the M -dimensional transmit symbol vector with $E[|\mathbf{s}_i|^2]$
 130 $= M^{-1}$, \mathbf{n} is the $\mathbb{C}^{M \times 1}$ additive independent and identically distributed (i.i.d.)
 131 circular symmetric complex Gaussian noise vector of $h_{i,j} \sim \mathcal{CN}(0, \sigma^2)$ with $\sigma^2 = N_0$
 132 and $\mathbf{r} = (r_1, r_2, \dots, r_N)^T$ is the transpose N -vector of received symbols. The set of
 133 all transmitted symbols form an M -dimensional complex constellation \mathcal{O}^M of P^M
 134 vectors, which specifies the dimensionality of the system.

2.2. MIMO Detection

135 The channel \mathbf{H} is assumed to be known at the receiver through a preceding training
 136 period. This generates and saves data in the channel estimation block regarding the
 137 modulation schemes and the channel condition statistics. MIMO algorithms solve
 138 (1) by separating parallel data streams transmitted by antennas. They can generally
 139 be categorized into four types as described below.

2.2.1. Maximum Likelihood (ML)

141 ML detection finds the minimum constellation point in (1) within the received
 symbols. It is given by

$$142 \quad \hat{\mathbf{s}}_{ML} = \arg \min_{\mathbf{s} \in \mathcal{O}^M} \|\mathbf{r} - \mathbf{H}\mathbf{s}\|^2 \quad (2)$$

143 The ML detector is optimal and fully exploits all available diversity. Even though ML
 144 produces the best BER performance, due to its use of exhaustive search, it can have
 145 immense complexity for direct implementation. The complexity grows exponentially

146 with the transmission rate R_c , since the detector needs to go through 2^{R_c} hypotheses
 147 for each received vector. For example, for the case of a 4×4 iterative-MIMO system
 148 employing 16-QAM, the detector would need to search a total of $K_s = 16^4 = 65536$
 149 candidates in order to find the correct transmitted vector. Several efficient subop-
 150 timal detection techniques have therefore been proposed or adapted from the field
 151 of multiuser detection. Even though these techniques are much less computationally
 152 demanding than the ML detector, they are often unable to exploit a large part of the
 153 available diversity, and thus, their performance tends to be significantly poorer than
 154 that of ML detection. However, this trade-off can be made for efficient hardware
 155 designs.

156 2.2.2. Zero Forcing (ZF) - Linear Detection

157 This method neglects the constraint $\mathbf{s} \in \mathcal{O}^M$ in (2) and uses different criteria to
 158 find the nulling vectors, the most common being the ZF or MMSE approach [*Golub*
 159 *and Loan*, 1983]. Generally, the symbol $\hat{\mathbf{s}}$ is given by a transformation of the received
 vectors \mathbf{r} in the form of

$$160 \quad \hat{\mathbf{s}} = Q(\mathbf{H}^+ \mathbf{r}) \quad (3)$$

161 where \mathbf{H}^+ is the Moore-Penrose pseudoinverse matrix that depends on channel \mathbf{H}
 162 and Q is a quantizer that maps the argument into the closest point in \mathcal{O}^M . Even
 163 though this method has low complexity, it does have a major drawback of having a
 164 rather poor performance in terms of BER.

165 2.2.3. V-BLAST - Ordered Successive Interference Cancellation

166 V-BLAST [*Golden et al.*, 1999] method, gives slightly better BER performance in
 167 comparison to linear detection. However, due to the error propagation, it is still
 168 suboptimal in performance. This is often overlooked due to its practicality during
 169 implementation. V-BLAST is a recursive procedure that works by minimizing the
 170 influence of noise by re-ordering the channel matrix according to the signal strength
 171 received. The algorithm simply makes a first detection of the most powerful signal,
 172 consequently subtracting that signal from the overall detected symbols. It then con-
 173 tinues the same process by proceeding to the detection of the second most powerful
 174 signal, and so forth. Assuming the ordered set to be

$$175 \quad \S \equiv \{k_1, k_2, \dots, k_M\} \quad (4)$$

176 the detection algorithm operates on \mathbf{r}_i , given in (5), while computing the decision
 177 statistics $y_{k_1}, y_{k_2}, \dots, y_{k_M}$, which are then quantized to form estimates of the received
 178 symbols $\hat{\mathbf{s}}_{k_1}, \hat{\mathbf{s}}_{k_2}, \dots, \hat{\mathbf{s}}_{k_M}$. The detection order is determined by the information about
 179 the channel conditions readily available within the estimation block. After computing
 180 (3), the detection process uses linear combinatorial nulling and symbol cancellation
 181 to successively compute the received vectors.

$$182 \quad \mathbf{r}_{i+1} = \mathbf{r}_i - \hat{\mathbf{s}}_{k_i}(\mathbf{H})_{k_i} \quad (5)$$

183 When combined with the ZF method, it shows some improvement in BER while
 184 still maintaining low complexity. The complete V-BLAST/ZF detection algorithm
 185 is summarized in Table 1, where \mathbf{G} denotes the Moore-Penrose pseudoinverse of the
 186 current channel \mathbf{H} , and therefore, $(\mathbf{G}_i)_j$ is the j^{th} row of \mathbf{G}_i , $Q(\cdot)$ is a quantizer

187 to the nearest constellation point, $(\mathbf{H})_{\bar{k}_i}$ is the k_i^{th} column of \mathbf{H} , $\mathbf{H}_{\bar{k}_i}$ denotes the
 188 matrix obtained by zeroing the columns k_1, k_2, \dots, k_i of \mathbf{H} , and $\mathbf{H}_{\bar{k}_i}^+$ denotes the
 189 pseudoinverse of $\mathbf{H}_{\bar{k}_i}$. This type of detection scheme is best deployed in high SNR
 190 environments.

191 2.2.4. Sphere Decoding (SD) and Fixed Sphere Decoding (FSD)

192 SD reduces the complexity of the ML detection problem [*Viterbo and Boutros,*
 193 1999] [*Pohst, 1981*] [*Agrell et al., 2006*] by introducing a constraint within the search
 called the sphere radius, R .

$$194 \quad \hat{\mathbf{s}}_{SD} = \arg \min_{\mathbf{s} \in \mathcal{O}^M} \|\mathbf{r} - \mathbf{H}\mathbf{s}\|^2 \leq R \quad (6)$$

195 The search can be visualized as a tree, traversing down each node until it encounters
 196 one with Euclidean Distance (ED) that is larger than R , where it will eliminate that
 197 branch from the search. The minimum symbol is acquired once it has traversed down
 198 through every path reaching the end i.e. the leaf node(s). The SD has major draw-
 199 backs when it comes to hardware implementation due to having variable complexity
 200 and its sequential nature. The complexity of the SD depends on the noise level and
 201 the channel conditions. Moreover, the linearity of the search prevents parallelism for
 202 newer hardware design implementation. Parallelization has been proven to minimize
 203 energy consumption in circuit designs due to a workload being shared across multiple
 204 computational resources, so that the circuit can produce the same amount of through-
 205 put at a lower frequency of operation. [*Chen et al., 2010*] [*Esmaeilzadeh et al., 2011*]
 206 [*Kumar et al., 2003*]. Therefore, [*Barbero and Thompson, 2008*] proposed a modified
 207 version, the FSD, in order to overcome both shortcomings. FSD is a combination of

brute-force enumeration and a low complexity, approximate detector. Much like the SD, FSD traverses down the tree whilst calculating the ED; however, instead of having a radius constraint R , FSD determines in advance the number of lattice points $\hat{\mathbf{s}}$ around received signal \mathbf{r} it would pass through, evaluating \mathbf{r} independent of the noise level, giving it a fixed throughput. The algorithm makes use of the fact that [Barbero and Thompson, 2008] the diagonal entries of \mathbf{R} from the \mathbf{QR} -decomposition of the channel matrix satisfy

$$E[\mathbf{r}_{11}^2] < E[\mathbf{r}_{22}^2] < \cdots < E[\mathbf{r}_{NN}^2] \quad (7)$$

Thus, the number of candidates at antenna level k denoted by n_k should follow

$$E[n_N] \geq E[n_{N-1}] \geq \cdots \geq E[n_1] \quad (8)$$

The main idea of FSD is to assign a fixed but distinct number of candidates to be searched per antenna level. The FSD is considered a promising algorithm for soft-MIMO detection. Since its introduction, the reduction of complexity in FSD has received significant attention [Barbero et al., 2008] [Lei et al., 2010] [Liu et al., 2011] [Li et al., 2009] [Wu and Thompson, 2011].

2.3. Iterative Decoding

An iterative decoder [Hagenauer et al., 1996] is used right after the MIMO symbols have been detected, where soft information extrinsic log-likelihood ratio (LLR) values are exchanged iteratively between the outer decoders with interleaving/de-interleaving operations in between until the desired performance is achieved [Berrou et al., 1993]. The idea behind soft detection is to generate *a posteriori* probability

(APP) values in the form of LLR information, $L_E(b_k|\mathbf{r})$, about the interleaved bits, \mathbf{b} , for $1 \leq k \leq K_e$, while taking into account the channel observations \mathbf{r} and the *a priori* LLR information, $L_A(b_k)$, coming from the outer decoder. For the system under consideration, assuming that the bits b_k are statistically independent due to the interleaving operation and making use of the Max-log approximation, $L_E(b_k|\mathbf{r})$ can be approximated by

$$L_E(b_k|\mathbf{r}) \approx \frac{1}{2} \max_{\mathbf{b} \in \mathcal{L} \cap \mathbb{B}_{k,+1}} \left(\frac{-\|\mathbf{r} - \mathbf{H}\mathbf{s}\|^2}{\sigma^2/2} + \mathbf{b}_{[k]}^T \mathbf{L}_{A[k]} \right) - \frac{1}{2} \max_{\mathbf{b} \in \mathcal{L} \cap \mathbb{B}_{k,-1}} \left(\frac{-\|\mathbf{r} - \mathbf{H}\mathbf{s}\|^2}{\sigma^2/2} + \mathbf{b}_{[k]}^T \mathbf{L}_{A[k]} \right) \quad (9)$$

for $1 \leq k \leq K_e$, where, without loss of generality, $K_e = M \cdot \log_2 P$ has been assumed to simplify the index notation. In (9), $\mathbf{b} = (b_1, b_2, b_3, \dots, b_{K_e})^T$, $\mathbf{b}_{[k]}$ denotes the subvector of \mathbf{b} omitting b_k , $\mathbf{L}_A = [L_A(b_1), L_A(b_2), \dots, L_A(b_{K_e})]^T$, $\mathbf{L}_{A[k]}$ denotes the subvector of \mathbf{L}_A omitting $L_A(b_k)$, $\mathbb{B}_{k,+1}$ and $\mathbb{B}_{k,-1}$ represent the sets of 2^{K_e-1} bit vectors \mathbf{b} having $b_k = +1$ (logical 1) and $b_k = -1$ (logical 0) respectively, $\mathcal{L} \cap \mathbb{B}_{k,+1}$ and $\mathcal{L} \cap \mathbb{B}_{k,-1}$ denote the subgroups of vectors of \mathcal{L} that have $b_k = +1$ and $b_k = -1$ respectively. The list of candidates $\mathcal{L} \subset \mathcal{O}^M$ is detector specific and subject to the overall performance and complexity of the iterative-MIMO receiver, since $\|\mathbf{r} - \mathbf{H}\mathbf{s}\|^2$ needs to be computed for all $\mathbf{s} \in \mathcal{L}$. Although iterative decoding does contribute to the overall complexity of a MIMO receiver, numerous studies have been done in reducing the total complexity of iterative decoding [Li et al., 2013] [Mathana et al., 2009] [Wu, 2011] [Zhongfeng et al., 2009], therefore, this paper focuses on minimizing energy consumption in the MIMO detector. It should be noted that

245 some of the complexity of iterative decoding will be avoided due to the proposed
 246 adaptive algorithm design; however, this is out of scope of this paper.

2.4. Power Savings

247 Energy consumption in mobile devices with battery powered sources is a major lim-
 248 iting factor in circuit designs. Fundamentally, energy is consumed in both dynamic
 249 and static aspects as specified by (10). Most publications like [*Mirsad et al.*, 2009],
 250 [*Andrei et al.*, 2009] and [*Salehi et al.*, 2009] have successfully reduce the dynamic
 251 power consumption, however, in newer chip technologies, the static power consump-
 252 tion is said to be high, [*Telikepalli et al.*, 2006], therefore, this work investigates ways
 253 to reduce both types, dynamic and static energy consumption, in a circuit design,
 254 while ensuring the algorithm performance is sufficient. This will ensure the adaptive
 255 algorithm is properly optimized to meet power budget of the design. In order to
 256 evaluate the overall power savings gained by the adaptive algorithm, both software
 and hardware savings should be analyzed.

$$257 \quad E_{total} = E_{dynamic} + E_{static} + E_{I/O} + E_{transceiver} \quad (10)$$

258 There are multiple ways to exploit energy savings in circuit designs and different
 259 energy has different approach to execute these. For example, savings in $E_{dynamic}$ are
 260 achieved by deploying the Dynamic Voltage and Frequency Scaling (DVFS) tech-
 261 nique [*Rabaey et al.*, 2009] while on the other hand, savings in E_{static} depend on the
 262 manufacturing process, the temperature, and the voltage, V .

2.4.1. Dynamic Energy

Dynamic energy, $E_{dynamic}$, spent within CMOS technology is due to toggling of transistors and is a function of clock frequency, f , which can be varied within some limit (before the circuit fails to function due to overheating), the value of V , and the capacitance. The $E_{dynamic}$ is given by the relation [Abusaidi et al., 2008] below

$$E_{dynamic} = \frac{nCV^2f}{t} \quad (11)$$

where n is the number of toggling transistors, C is the circuit capacitance, V is the voltage swing, f is the toggling frequency and t is the time it takes to complete an operation. DVFS has shown significant energy savings when applied to circuit designs, evident in [Larson and Gustafsson, 2011], [ARM Industry, 2009] and [Kim et al., 2008]. Much like the adaptive algorithm, DVFS has the ability to adjust its parameters to match the computational demand of the current workload. If the workload requirement is high, DVFS will increase the V , to supply the circuit so that it can operate at a higher f in order to meet the desired data throughput within a particular time period. The opposite is also true; when the workload is minimal, the circuit could operate on a much lower f , which ultimately, according to (11) will decrease the overall $E_{dynamic}$ as the task time lengthens. This adaptivity is appealing to the design of the adaptive algorithm since now both hardware and software possess the same level of adaptivity and ‘intelligence’. Both approaches will in turn yield significant overall energy savings.

2.4.2. Static Energy

Static energy, E_{static} , is consumed due to transistor leakage and is highly dependent on the manufacturing process, the ambient temperature of the circuit, and the value

285 of V . According to the study by [*Telikepalli et al.*, 2006], E_{static} seems to dominate the
286 overall power consumption within a circuit as the chip size shrinks. Therefore, E_{static}
287 can no longer be neglected when designing new algorithms into new chip technology.

3. Adaptive Algorithm Methodology

288 Current MIMO detectors usually lack adaptivity whereby all receivers behave ex-
289 actly the same way regardless the received signal characteristics. This ‘one size fit all’
290 architecture does not work well in some situations, since different users experience
291 distinct channel conditions. For example, a stationary user who is physically near
292 to a transmitter would often have a better data throughput than one who is further
293 away. Doppler rates determined by motion in the environment also play a part in
294 determining the current condition of the channel. To decode symbols in bad channel
295 conditions would prove to be pointless since the data would not be likely to be de-
296 coded successfully anyway. Therefore, having ‘intelligence’ in the detector that could
297 modify its behavior according to current channel conditions would be ideal. This
298 adaptivity in the algorithm is controlled by the MI calculation between the transmit-
299 ters and receivers. It is well-known that MI of a MIMO channel is given by (12) and
300 the information required, \mathbf{H} is already available within the channel estimation block.
301 Different values of initial received soft information may lead to significantly different
302 behavior during the iterative decoding process. The study done by [*Zhang et al.*,
303 2009], which compares the performance of iterative decoders using different received
304 soft LLR information metrics, discovered that by computing the MI, the number of

305 iterations in turbo decoding can be found using the highest complexity ML MIMO
 306 detection method. [Zhang *et al.*, 2009] also proves that the best approximation of the
 307 received symbols obtained are lossless and that the exact LLR values are sufficient
 308 enough statistic of \mathbf{r} about \mathbf{s} . Therefore, using this information and the principle of
 309 exploiting MI calculation in (12), the paper applies this approach for the first time to
 310 a MIMO detector to further save energy consumption in the overall receiver. With
 311 any given channel model in (1), and a Gaussian constellation with $E[|\mathbf{s}_i|^2] = M^{-1}$,
 the MI for the ML method is

$$312 \quad \bar{I}(\mathbf{H}_k) \triangleq \log_2 \det\left(I + \frac{\mathbf{H}_k \mathbf{H}_k^T}{N_0}\right) \quad (12)$$

313 The values of MI spread at specific SNR conditions. Figure 2 illustrates the accumu-
 314 lated MI performance of the detector as a function of probability of receiver fails and
 315 successes. The system is simulated using a 4×4 MIMO system with 16-QAM modula-
 316 tion symbols transmitting 1024 bits per packet of 10000 channel realizations utilizing
 317 an iterative-MIMO decoder of $1/2$ code rate in a fast fading environment. Threshold 1
 318 can be obtained in Figure 2(a), which shows the FSD performance. Below a certain
 319 MI threshold of approximately 2200, the receiver is certain to fail when trying to
 320 decode a symbol message. Therefore, the best cause of action for the receiver is to
 321 request a retransmission i.e. Automatic Repeat Request (ARQ), from the transmitter
 322 rather than to attempt decoding where it is unlikely to succeed, wasting significant
 323 computational energy, which is the limitation of today's system designs. On the
 324 other hand, the V-BLAST/ZF performance is shown in Figure 2(b), where a value of
 325 about 7100 for threshold 2 can be seen. The receiver will decode the symbol message

326 with very high probability above this MI value, therefore, a simpler detection method
327 will suffice in detecting the symbol, i.e. the V-BLAST/ZF method. In addition, the
328 area in-between the two thresholds shows that the receiver would sometimes fail to
329 decode. Thus, a more powerful detection method is needed to assist the receiver in
330 decoding the message. This is done by deploying the FSD algorithm in the MIMO
331 detector. By obtaining these thresholds, the design of the adaptive algorithm can be
332 described in Table 2. It should be noted that, the thresholds obtained are catered
333 specifically for 16-QAM modulation scheme on a 4×4 MIMO system, however, the
334 idea behind adaptive algorithm can be adjusted to fit any communication systems.
335 The same analysis can be applied to all other modulation and coding schemes, with
336 the exception of having different threshold values when calculated using (12).

4. Results and Analysis

337 The effectiveness of the adaptive algorithm can be measured using the performance
338 and complexity trade-off metrics. This section describes these efficiencies from both
339 hardware and software perspectives.

4.1. SOFTWARE - Performance

340 The performance can be quantified by calculating the number of errors in a total
341 frame i.e. the BER analysis. The system design has been set to tolerate a BER of
342 10^{-3} or less in high SNR regions. In the system model used, the BER is depicted
343 in Figure 3. The adaptive algorithm gives similar performance to the FSD and
344 performs much better than the V-BLAST/ZF algorithm in low SNR regions. In very

345 high SNRs, i.e. 10 dB and above, the less complex algorithm of V-BLAST/ZF is
346 adopted and the BER performance is below the set error tolerance line. The FSD
347 does give a much better performance than the tolerance line, however, this level of
348 performance is unnecessary and only adds extra complexity for the hardware. When
349 the SNR is below 0 dB, the receiver abandons the detection process (subsequently
350 avoiding the complexity of the iterative decoding process as well, gaining substantial
351 power savings) and requests a retransmission from the transmitter, whereas the area
352 above the set threshold, circa 0 dB to 6 dB, the adaptive algorithm provides much
353 higher chances of successful processing in comparison to the V-BLAST/ZF method.

4.2. SOFTWARE - Complexity

354 By obtaining the thresholds, the total number of usage of each MIMO detection
355 algorithm throughout the span of the SNR is shown in Figure 4, depicting transmis-
356 sions of 10000 packets of 1024 bits per frame. It clearly shows that below an SNR
357 value of 0 dB i.e. threshold 1, no processing is taking place. In addition, in high
358 SNR regions, V-BLAST/ZF is utilized. This figure concurs with Figure 3, where the
359 performance coincides with the algorithm switching rate of successfulness. From this,
360 another part of the parameter, the complexity measurement of the software can be
361 determined.

362 Complexity measurement gives an important overview of the hardware before im-
363 plementation and provides an initial indication of power savings in the design. A
364 preliminary complexity analysis of the adaptive algorithm is determined by the mul-
365 tiplier counts in the code. Assuming that the complexity of channel ordering is the

366 same for both detection schemes, the multiplier counts between the FSD and V-
 367 BLAST/ZF detection schemes for a transmission of one symbol for 4×4 M-QAM
 368 deploying FSD is M -times more complex than the V-BLAST/ZF. Figure 5 plots the
 369 percentage complexity results against the SNR of the channels, where 100% equals
 370 the complexity of FSD, while the V-BLAST/ZF requires only 25%. The complexity
 371 of the adaptive algorithm can be calculated by averaging over MI values shown at
 372 certain SNR in the figure and it is much lower than the FSD, i.e. 62% of the multi-
 373 pliers required. Most energy savings can be gained during the 'No Decoding' phase
 374 since no processing is required in this region. Furthermore, energy are saved during
 375 the utilization of V-BLAST/ZF algorithm i.e. where $MI > 7100$, which gives a total
 376 of only 25% multiplier usage.

4.3. HARDWARE - Performance and Complexity

377 Xilinx®Virtex-5 has a varying voltage range of 0.95 V to 1.05 V, and an opera-
 378 tional frequency range of 60 MHz to 400 MHz [Klein, 2009]. In order to assess the
 379 efficacy of the DVFS technique in saving energy consumption in wireless communi-
 380 cation, both MIMO detection algorithms - FSD and V-BLAST/ZF, are operated at
 381 low power mode (0.95 V, 60 MHz) and high performance mode (1.05 V, 400 MHz)
 382 to get the minimum and maximum thresholds of operation. This information is de-
 383 termined using the Xilinx®Design Suite software for the Xilinx®Virtex-5. The Xil-
 384 inx®Design Suite software comprises a co-design software/hardware setup performed
 385 in Matlab™ and Xilinx®System Generator, which is a part of the Xilinx®ISE. In
 386 addition, the power profile is analyzed using the Xilinx®Power Estimator (XPE)

387 tool. The summary of the total number of the FPGA resources used are given in
 388 Table 3. The percentage of slices used can be seen as an indicator of the amount of
 389 control logic and intermediate buffers required in the adaptive algorithm. This factor
 390 affects hardware mapping and the resulting throughput. The average throughput of
 391 the system is a parameter of importance when considering the performance of the
 392 algorithm. The throughput in megabits per second (Mbps) is calculated according
 393 to

$$394 \quad Q_{avg} = M \cdot \log_2 P \cdot f / C_{avg} \quad (13)$$

395 where C_{avg} is the average number of clock cycles required to detect a MIMO symbol.

396 For low power mode, where $f = 60$ MHz and the minimum number of cycles is
 397 $C_{min} = 4$, the maximum throughput is $Q_{min} = 240$ Mbps while the high performance
 398 mode gives a throughput of $Q_{max} = 1200$ Mbps. Increasing the clock frequency would
 399 result in a significant increase in the throughput, therefore, the $f = C_{avg}$ could be
 400 seen as an indicator of the level of optimization of the hardware design. The hardware
 401 setup parameters are included in Table 4.

402 Similar to details reported in [Mirsad et al., 2009] [Andrei et al., 2009] [Salehi et al.,
 403 2009] [Larson and Gustafsson, 2011], there are significant dynamic power savings in
 404 the circuit, portrayed in Figure 6, where low power mode uses 9% of the overall power
 405 in comparison to 29% when the circuit is run at full power i.e. the high performance
 406 mode. However, these savings would be minimal in comparison due to the much
 407 larger static power, which dominates the overall chip power. Figure 7 shows the
 408 low power results for FSD (a) and V-BLAST/ZF (c) as well as the high performance

409 statistics, (b) and (d), for FSD and V-BLAST/ZF respectively. It is shown that some
410 savings are gained when the adaptive algorithm switches from the high complexity
411 FSD to the simpler V-BLAST/ZF detection. The power saved during the swap is
412 equivalent to 20% for high performance and 8% for low power mode. The energy
413 savings when changing from high performance to low power are also illustrated here.
414 The total time computed is obtained by transmitting one packet of 1024 bit frame
415 using a 16-QAM modulation symbol over the 4×4 MIMO channel when operating at
416 the lowest frequency of 60 MHz. When operating at 400 MHz, the task completion
417 time takes approximately 7 times less than when operating at lower frequency. By
418 finishing quickly, the hardware can be put into sleep mode, reducing the total energy,
419 since the idle power is negligible ≈ 0.08 mW. By calculation, at the same total rate
420 of completion, the energy required to complete one task is lower by 42% when the
421 circuit operates quickly and switches into idle state (high performance) than to run
422 slowly and finishes just in time, at lower frequency (low power) when deploying FSD,
423 and 52% for the V-BLAST/ZF algorithm. These are the savings which can be gained
424 when putting the chip into sleep mode for more than $15 \mu\text{s}$. Even though in theory,
425 verified in (11), the longer the task runs, the lower the dynamic energy consumption,
426 this is not the case here because when evaluating the total energy consumption of
427 the circuit, the E_{static} required in powering up the Xilinx®Virtex-5 hardware is too
428 large, occupying most of the power demand of the chip, resulting in 84% and 65% of
429 the total power for low power and high performance mode respectively, as shown in
430 Figure 6. These findings coincide with the work reported in [*Hasan and Bird, 2011*];

431 stating that, as manufacturing process get smaller, the E_{static} seems to dominate
432 the overall chip power. Therefore, it can be concluded that running the circuit at
433 a lower speed is not the answer to overall power savings in this technology. E_{static}
434 could no longer be neglected when designing a circuit, and it is now more essential to
435 take temperature as a parameter in saving overall energy consumption, since E_{static}
436 strongly depends on the heat generated by the circuit.

437 Figure 8 shows the overview of the algorithm flow within the chip. Only one
438 detector is switched on at any given time according to the calculation from the
439 threshold control block. This is particularly useful for FPGA implementation since
440 the hardware resources are switched on and off as required. The implementation of
441 the adaptive algorithm is illustrated in terms of the FPGA hardware given in Figure
442 9. The configurable logic utilised for each detector is shown in (a) for FSD, (b) for
443 V-BLAST/ZF and (c) when ‘No Decoding’ is taken place. It can be seen that only
444 certain parts of the overall chip hardware are turned on at any given time. Seeing
445 that most power consumption is due to powering the up the chip itself, i.e. static
446 power, the adaptive algorithm takes advantage of this fact and therefore shuts down
447 parts of the chip which are not in use. To show how the adaptive algorithm behaves,
448 consider four extreme scenarios of three frames of 1024 data bits per frame size being
449 transmitted over different environments, where T_1 is when the MI is at a high value,
450 T_2 is for when MI is acceptable and T_3 is for MI being low and not suitable for
451 further decoding. From Figure 5, it is shown that, the complexity of an FSD is four
452 times larger than that of the V-BLAST/ZF. Therefore, if the complexity of the V-

453 BLAST/ZF is set to 1, the FSD will have the equivalent complexity of 4. The overall
 454 chip area usage is given in Figure 10. Using the same complexity ratio, consider a
 455 transmission of 100000 frames of 1024 bits per frame on random fast fading channel
 456 realisations over various ranges of SNR values from -4 dB to 20 dB. The adaptive
 457 algorithm saves approximately 30% of the overall resource in comparison to the FSD
 458 detector whilst maintaining the BER performance at a satisfactory region.

459 Shutting down parts of the chips i.e. sleep modes, are the key enablers in saving
 460 further energy in the design on Virtex-5 hardware. By running the circuit at high
 461 frequency, the sleep modes can help prevent the circuit from running and powering
 462 up the entire logic gates all the time, consequently preventing the circuitry from
 463 overheating that leads to high E_{static} consumption.

464 For greater insight of the total energy savings that can be achieved in a realistic
 465 setting, Figure 11 considers the adaptive algorithm in a Rayleigh fading channel.
 466 The SNR chosen are based on the operating SNR regions of the Long Term Evo-
 467 lution (LTE). In small cells, the transmit power is to be in the range of 23 dB to
 468 46 dB, averaging at 26.5 dB [Nakamura, et al., 2013]. The savings can found by
 469 integrating the power, P , with respect to the probability density function, f , of the
 470 fading environment, ρ , as shown in (14).

$$\int_a^b P(\rho)f(\rho) d\rho \quad (14)$$

471 where a is the lower SNR value of -4 dB and b is the upper limit of the SNR, which
 472 is 40 dB in this case. Using a discrete approximation to this gives a measure of

473 the savings that can be achieved in practice. For example, taking the FSD as a
474 benchmark would use 8 J (in high performance) of energy to decode the 1024 bits
475 data packet size. Utilizing the adaptive algorithm would use 70% less resources since
476 the FSD does not take into account the transmit power nor the SNR values, which
477 results in unnecessary power wastage. In addition, the behavior of the adaptive
478 algorithm follows that of the Rayleigh fading channel for a 4×4 MIMO system,
479 operating on 74% of the fading channel environment, gaining energy savings due to
480 sleep implemented in the appropriate regions i.e. FSD is on sleep mode at SNR of
481 20 dB, and only V-BLAST is active.

482 The energy saving results obtained can be optimized further by combining the
483 common circuitry of the FSD and V-BLAST since they share some common func-
484 tionality. By sharing the circuitry resources between the two algorithms can gain
485 additional energy savings. Detailed evaluation of the issues is the next major step of
486 the project.

5. Future Direction

487 Research is still ongoing in the field of both hardware and software design. This
488 section describes some of the planned future work.

5.1. SOFTWARE - Algorithm Switching Selection

489 The SNR values at which the adaptive algorithm switches between the different
490 thresholds is illustrated in Figure 4. The selection of adaptive algorithm can be
491 optimized. At a particular SNR, the MI varies, and must be calculated by the

492 receiver. The effect is that the detector switches between approaches in regions
493 corresponding to the MI thresholds. The transitions across the MI thresholds result
494 in switching from one to the other rapidly. This switching could have an impact on
495 the power consumption. One possible improvement is to enforce use of FSD during
496 these situations when V-BLAST/ZF fails to decode a packet, or when there would
497 be rapid switching between FSD and ‘No Decoding’. However, even though this
498 would increase the likelihood of decoding, it would be at a cost of higher energy
499 consumption.

5.2. HARDWARE - New Xilinx®Virtex 7

500 Newer technology chips such as the Xilinx®Virtex-7, based on a different manufac-
501 turing process, have an improved solution to the high E_{static} consumption of previous
502 circuit technologies [Hussein et al., 2013]. It may therefore be that DVFS can be
503 applied to minimize power consumption in this type of hardware, due to E_{static} no
504 longer dominating the total chip power.

6. Conclusion

505 Having ‘intelligence’ in the algorithm design and the hardware offers both adequate
506 performance and reduced complexity in future iterative-MIMO systems. The adap-
507 tive algorithm within the MIMO receiver demonstrates significant energy savings in
508 both software and hardware implementation. It has the potential to save up to 30%
509 energy in the software design and in the Xilinx®Virtex-5 hardware. This can be im-

510 proved further when incorporating sleep modes to reduce the E_{static} in the hardware
511 apparatus.

512 **Acknowledgments.** This work is funded by the University of Tun Hussein Onn
513 Malaysia as a part of the main author's PhD program.

References

514 Abusaidi, B. P., M. Klein, and B. Philofsky, Virtex-5 FPGA System Power Design
515 Considerations (2008), *White Paper*, vol. 285, pp. 1-23.

516 Agrell, E., T. Eriksson, A. Vardy, and K. Zeger, Closest Point Search in Lattices
517 (2002), *IEEE Transactions on Information Theory*, vol. 48, no. 8, pp. 2201-2214.

518 Andrei, A., P. Eles, Z. Peng, S. Link, M. Schmitz, and B. M. Al-Hashimi, Energy
519 Optimization of Multiprocessor Systems on Chip by Voltage Selection (2009), *IEEE*
520 *Transactions on Very Large Scale Integration (VLSI) Systems*, vol. 15, no. 3, pp.
521 262-275.

522 Ariyavisitakul, S.L, Turbo Space-Time Processing to Improve Wireless Channel Ca-
523 pacity (2000), *IEEE Transactions on Communications*, vol. 48, no. 8, pp. 1347-
524 1359.

525 ARM Industry, The ARM Cortex-A9 Processors (2009), *White Paper*, pp. 1-11.

526 Barbero, L.G., T. Ratnarajah, and C. Cowan, A low-complexity soft-MIMO detector
527 based on the fixed-complexity sphere decoder (2008), *IEEE International Confer-*
528 *ence on Acoustics, Speech and Signal Processing*, pp. 2669-2672.

- 529 Barbero, L.G., J. S. Thompson, Extending a Fixed-Complexity Sphere Decoder to
530 Obtain Likelihood Information for Turbo-MIMO Systems (2008), *IEEE Transac-*
531 *tions on Vehicular Technology*, vol. 57, no. 5, pp. 2804-2810
- 532 Barbero, L.G., J. S. Thompson, Fixing the Complexity of the Sphere Decoder for
533 MIMO Detection (2008), *IEEE Transactions on Wireless Communications*, vol. 7,
534 no. 6, pp. 2131-2142.
- 535 Berrou, C., A. Glavieux, and P. Thitimajshima, Near Shannon Limit Error - Correct-
536 ing Coding and Decoding: Turbo Codes (1993), *IEEE International Conference on*
537 *Communications*, no. 1, pp. 1064-1070.
- 538 Chen, Y.K, C. Chakrabarti, and B. Bougard, Signal Processing on Platforms with
539 Multiple Cores: Part 2 – Applications and Design (2010), *IEEE Signal Processing*
540 *Magazine*, vol. 2, no. 1, pp. 20-21.
- 541 Esmailzadeh, H., E. Blem, R. St. Amant, K. Sankaralingam, and D. Burger, Dark
542 Silicon and the end of Multicore Scaling (2011), *Proceeding of the 38th Annual*
543 *International Symposium on Computer Architecture*, pp. 365.
- 544 Fincke, B. U., M. Pohst, Improved Methods for Calculating Vectors of Short Length in
545 a Lattice, Including a Complexity Analysis (1985), *Mathematics of Computations*,
546 vol. 44, no. 170, pp. 463-471.
- 547 Golden, G.D, C. J. Foschini, R. A. Valenzuela, and P. W. Wolniansky, Detection Al-
548 gorithm and Initial Laboratory results using V-BLAST space time Communication
549 Architecture (1999), *IEEE Electronic Letters*, vol. 35, no. 1, pp. 14-16

- 550 Goldsmith, A., E. Biglieri, R. Calderbank, A. Constantinides, A. Paulraj, and H. V.
551 Poor (2007), *MIMO Wireless Communications*, Cambridge, Cambridge University
552 Press, pp. 1–559.
- 553 Golub, G. H., C. F. Van Loan, *Matrix Computations* (1983), Third. Baltimore and
554 London: The Johns Hopkins University Press, pp. 292-300.
- 555 Hagenauer, J, E. Offer, and L. Papke, Iterative decoding of binary block and convo-
556 lutional codes (1996), *IEEE Transactions on Information Theory*, vol. 42, no. 2,
557 pp. 429-445.
- 558 Hasan, M. Z., M. Bird, Energy Reductions for Embedded Processors in Reconfig-
559 urable Hardware (2011), *IEEE International Conference on Electro/Information*
560 *Techonology*, pp. 1-8.
- 561 Hochwald, B. M., and S. T. Brink (2003), Achieving Near-Capacity on a Multiple-
562 Antenna Channel *IEEE Transactions on Communications*, vol. 51, no. 3, pp. 389–
563 399.
- 564 Hussein, B. J., M. Klein, and M. Hart, Lowering Power at 28 nm with Xilinx®7
565 Series Devices (2013), vol. 389, pp. 1-25
- 566 Jaldén, J., L. G. Barbero, B. Ottersten, and J. S. Thompson, The Error Probabil-
567 ity of the Fixed-Complexity Sphere Decoder (2009), *IEEE Transaction in Signal*
568 *Processing*, vol. 57, no. 7, pp. 2711-2720.
- 569 Kim, W., M. S. Gupta, G. Wei, and D. Brooks, System Level Analysis of Fast,
570 Per-Core DVFS using On-Chip Switching Regulators (2008), *High Performance*
571 *Computer Architecture, IEEE 14th International Symposium*, no. 1620, pp. 123-

572 134.

573 Klein, M., Power Consumption at 40 and 45 nm (2009), *White Paper*, vol. 298, pp.
574 1-21.

575 Kumar, R., K. I. Farkas, N. P. Jouppi, P. Ranganathan, and D. M. Tullsen, Single-
576 ISA Heterogeneous Multi-Core Architectures: The Potential for Processor Power
577 Reduction (2003), *Proceedings of the 36th International Symposium on Microar-*
578 *chitecture*.

579 Larson, E. G., O. Gustafsson, The Impact of Dynamic Voltage and Frequency Scal-
580 ing on Multicore DSP Algorithm Design The Impact of Dynamic Voltage and
581 Frequency Scaling on Multicore DSP Algorithm Design (2011), *IEEE Signal Pro-*
582 *cessing Magazine*, no. 28.

583 Lei, S., Q. Tu, D. Yang, and J. Chen, Probabilistic tree pruning for fixed-complexity
584 sphere decoder in MIMO systems (2010), *International Conference on Wireless*
585 *Communications and Signal Processing (WCSP)*, pp. 1-6.

586 Li, G., X. Zhang, S. Lei, C. Xiong, and D. Yang, An Early Termination-based Im-
587 proved Algorithm for Fixed-complexity Sphere Decoder (2012), *IEEE Wireless*
588 *Communications and Networking Conference: PHY and Fundamentals*, no. 1, pp.
589 629-634.

590 Li, P., D. Paul, R. Narasimhan, and J. Cioffi (2006), On the Distribution of SINR
591 for the MMSE MIMO Receiver and Performance Analysis, *IEEE Transactions on*
592 *Information Theory*, vol. 52, no. 1, pp. 271-286.

- 593 Li, Liang, Maunder, Robert G., Al-Hashimi, Bashir, Hanzo, Lajos, A Low-
594 Complexity Turbo Decoder Architecture for Energy-Efficient Wireless Sensor Net-
595 works (2013), *IEEE Transactions on Very Large Scale Integration*, vol. 21, no. 1,
596 14-22.
- 597 Liu, L., J. Lofgren, and P. Nilsson, Low Complexity Soft-output Signal Detector for
598 Spatial-multiplexing MIMO system (2011), *IEEE International Wireless Commu-
599 nications and Mobile Computing Conference*, pp. 988–993.
- 600 Matthaiou, M., Laurenson, D.I., Wang, C.X, Reduced Complexity Detection for
601 Ricean MIMO Channels Based on Channel Number Thresholding (2008), *IEEE
602 22nd International Symposium on Personal, Indoor and Mobile Radio Communi-
603 cations*, pp. 1718–1722.
- 604 Mathana, J. M., P. Rangarajan, J. Raja Paul Perinbam, Low Complexity Recon-
605 figurable Turbo Decoder for Wireless Communication Systems (2013), *Arabian
606 Journal for Science and Engineering*, vol. 38, no. 10, pp. 2649–2662.
- 607 Mirsad, C., D. Persson, and E. G. Larson, Allocation of Computational Resources
608 for Soft MIMO Detection (2011), vol. 5, no. 8, pp. 1451-1461.
- 609 Nakamura, T., Trends in Small Cell Enhancements in LTE Advanced (2013), *IEEE
610 Communication Magazine*, vol. 51, no. 2, pp. 98–105.
- 611 Pohst, M., On the Computation of Lattice Vectors of Minimal Length, Successive
612 Minima and Reduced Bases with Applications (1981), *Newsletter ACM SIGSAM
613 Bulletin*, vol. 15, no. 1, pp. 37-44.

- 614 Rabaey, J., *Low Power Design Essentials* (2009), Department. New York: Springer
615 2009, pp. 289-316.
- 616 Salehi, M. E., M. Samadi, M. Najibi, A. Afzali-Kusha, M. Pedram, and S. M.
617 Fakhraie, Dynamic Voltage and Frequency Scheduling for Embedded Processors
618 Considering Power/Performance Tradeoffs (2011), *IEEE Transactions on Very*
619 *Large Scale Integration (VLSI) Systems*, vol. 19, no. 10, pp. 1931-1935.
- 620 Sellathurai, M., S. Haykin, TURBO-BLAST for Wireless Communications: Theory
621 and Experiments (2002), *IEEE Transactions on Signal Processing*, vol. 50, no. 10,
622 pp. 2538–2546.
- 623 Telikepalli, A., Power vs . Performance: The 90 nm Inflection Point Reducing Power
624 in FPGAs The Triple Challenge (2006), *White Paper*, vol. 223, pp. 1-18
- 625 Viterbo, E., J. Boutros, A Universal Lattice Code Decoder for Fading Channels
626 (1999), *IEEE Transactions on Information Theory*, vol. 45, no. 5, pp. 1639-1642.
- 627 Winters, J. H., S. Member, J. Salz, R. D. Gitlin, The Impact of Antenna Diversity
628 on the Capacity of Wireless Communication Systems (1994), *IEEE Transactions*
629 *on Communications*, vol. 42, no. 2, pp. 1740-1751.
- 630 Wu, P. H. Y., On the complexity of Turbo Decoding Algorithms (2001), *IEEE Ve-*
631 *hicular Technology Conference*, vol. 53, no. 2
- 632 Wu, X., J. S. Thompson, A Fixed-Complexity Soft-MIMO Detector via Parallel Can-
633 didate Adding Scheme and its FPGA Implementation (2011), *IEEE Communica-*
634 *tions Letters*, vol. 15, no. 2, pp. 241-243.

635 Zhang, J., M. A. Armand, P. Y. Kam, and A. T. Mi, A Mutual Information Approach
636 for Comparing LLR Metrics for Iterative Decoders (2009), *IEEE Communication*
637 *Society*, vol. 1, no. 4, pp. 1-4.

638 Zhang, J., M. A. Armand, P. Y. Kam, A. T. Mi, Low hardware complexity parallel
639 turbo decoder architecture (2009), *International Symposium on Proceedings of the*
640 *Circuits and Systems*, vol. 1, no. 4, pp. 1-4.

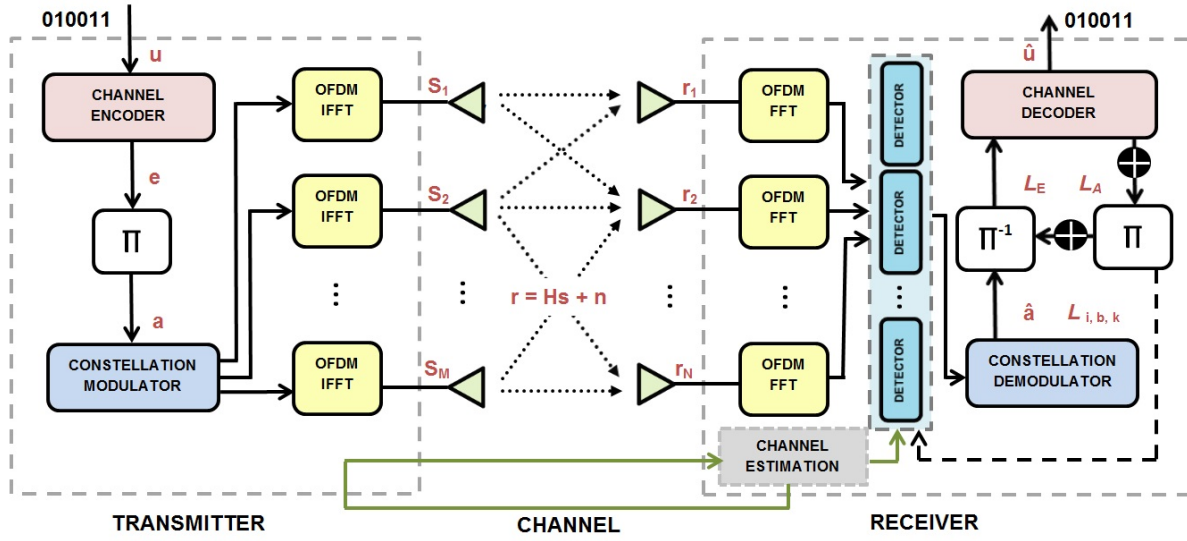


Figure 1. Iterative-MIMO (BICM) System

Table 1. V-BLAST/ZF Algorithm

Pseudo-Code

Channel realization:

$$\mathbf{G}_1 = \mathbf{H}^+$$

$$i = 1$$

Recursion:

$$k_i = \arg \min_{j \notin \{k_1, \dots, k_{i-1}\}} \| (\mathbf{G}_i)_j \|^2$$

$$y_{k_i} = (\mathbf{G}_i)_{k_i} \mathbf{r}_i$$

$$\hat{\mathbf{s}}_{k_i} = Q(y_{k_i})$$

$$\mathbf{r}_{i+1} = \mathbf{r}_i - \hat{\mathbf{s}}_{k_i} (\mathbf{H}_{k_i})$$

$$\mathbf{G}_{i+1} = \mathbf{H}_{k_i}^+$$

$$i = i + 1$$

641 ¹ Algorithm consists of channel ordering given by Line 3; Line 4 performs nulling and computes the decision statistic;

642 Line 5 quantizes the computed decision statistic to yield the decision; Line 6 performs cancellation by decision feedback, and

643 Line 7 computes the new pseudoinverse for the next iteration.

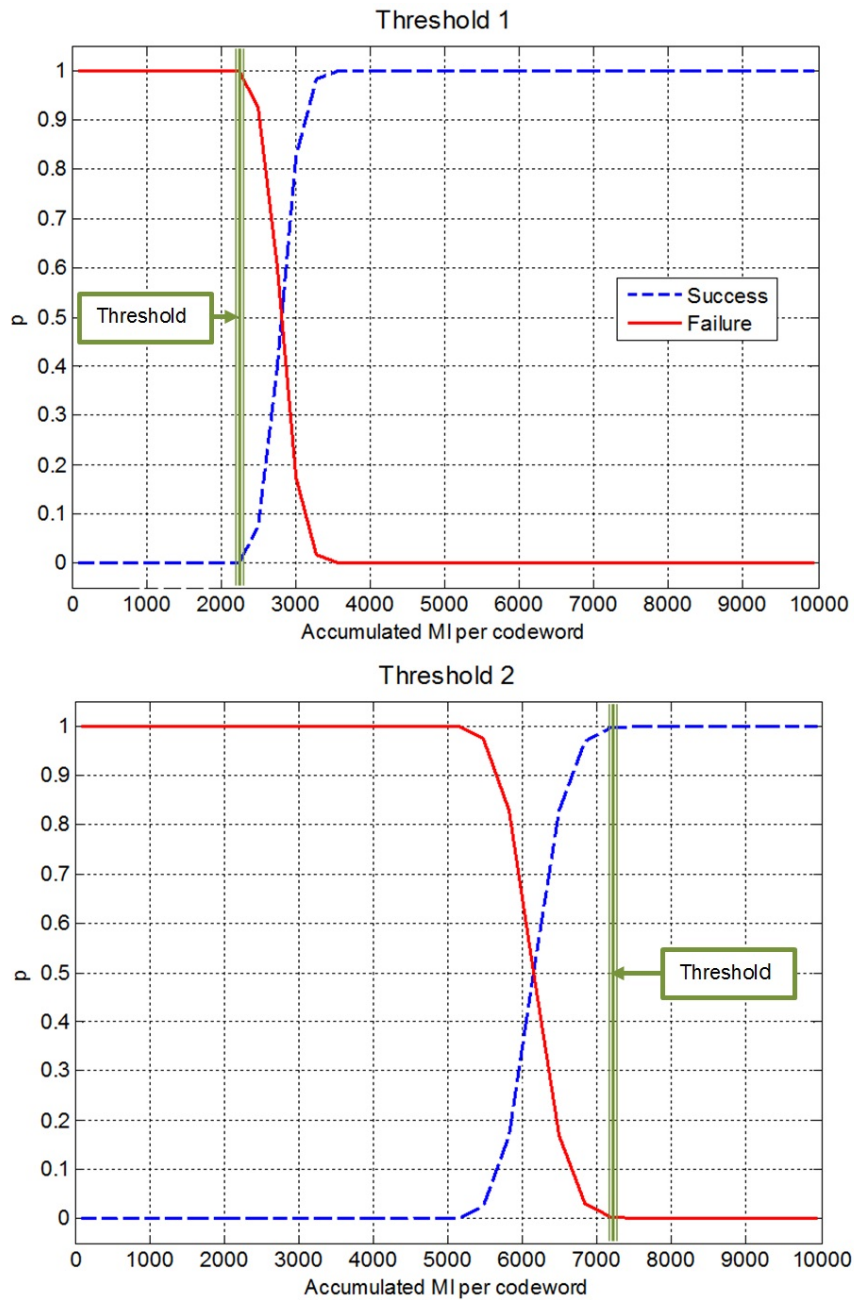


Figure 2. Probability of Receiver Successes and Failures on 4×4 MIMO where threshold 1 (a) is for FSD method and (b) is threshold 2, for V-BLAST/ZF method

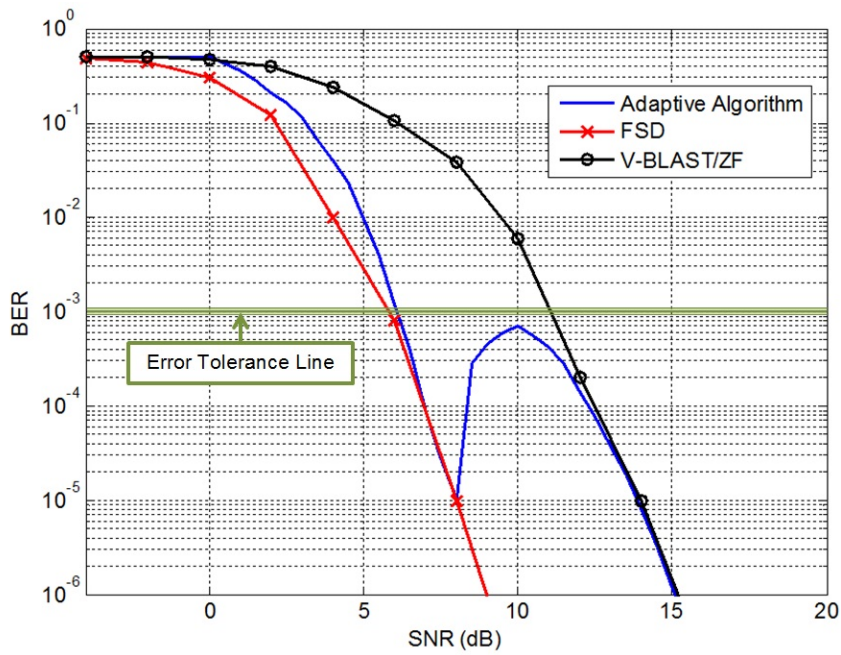


Figure 3. Performance Measurement of BER on Complex 4×4 MIMO System

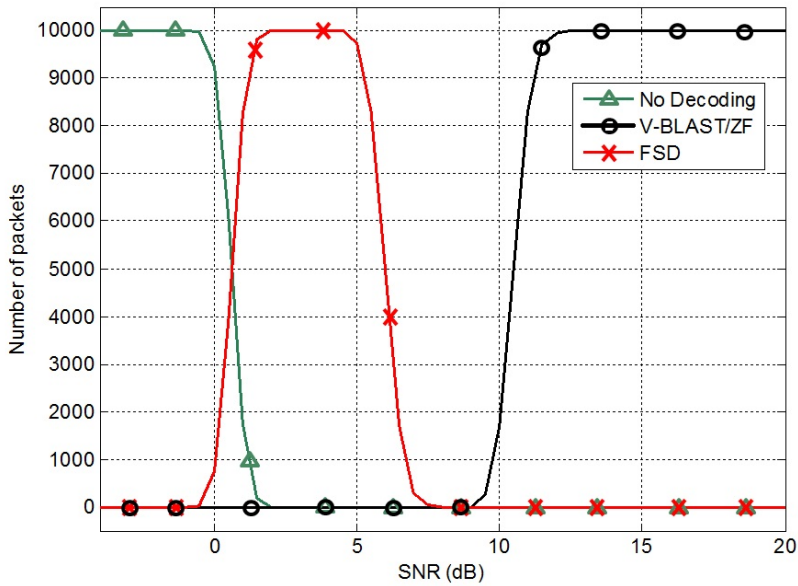


Figure 4. Algorithm Switching Selection in Receiver

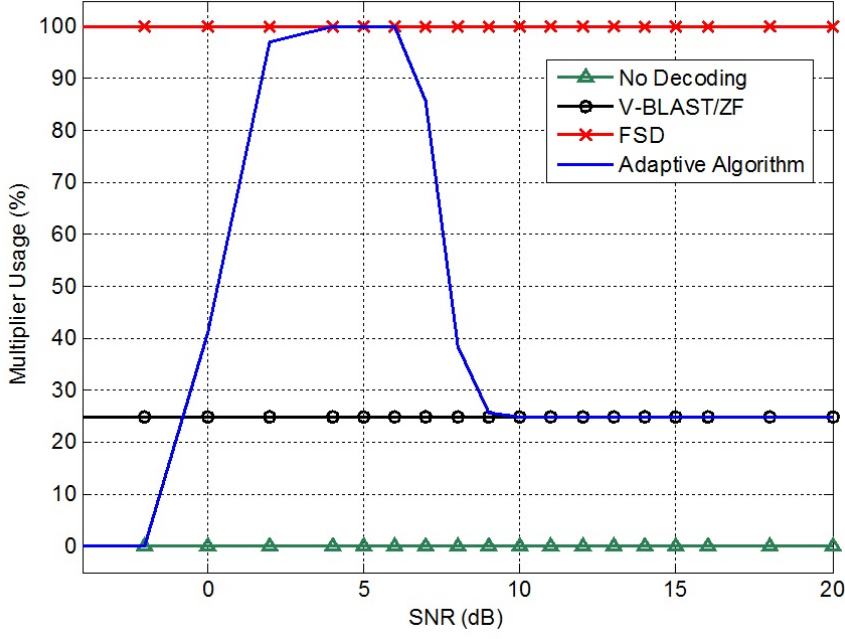


Figure 5. Complexity Measurements of Multiplier Counts between Different MIMO Detection Schemes

Table 2. Adaptive Algorithm

Pseudo-Code

Channel realization: $\{\mathbf{H}_1, \mathbf{H}_2, \dots, \mathbf{H}_k\}$

for $\mathbf{r}_i \leq \mathbf{r}_k$

$$\bar{I}(\mathbf{H}_k) \triangleq \log_2 \det\left(I + \frac{\mathbf{H}_k \mathbf{H}_k^T}{N_0}\right)$$

if $\bar{I}_i \leq \text{Threshold 1}$

\mathbf{r}_i error, request retransmission

elseif $\text{Threshold 1} \leq \bar{I}_i \leq \text{Threshold 2}$

\mathbf{r}_i with low MI : FSD

else $\bar{I}_i \geq \text{Threshold 2}$

\mathbf{r}_i with high MI : V-BLAST/ZF

endif

endfor

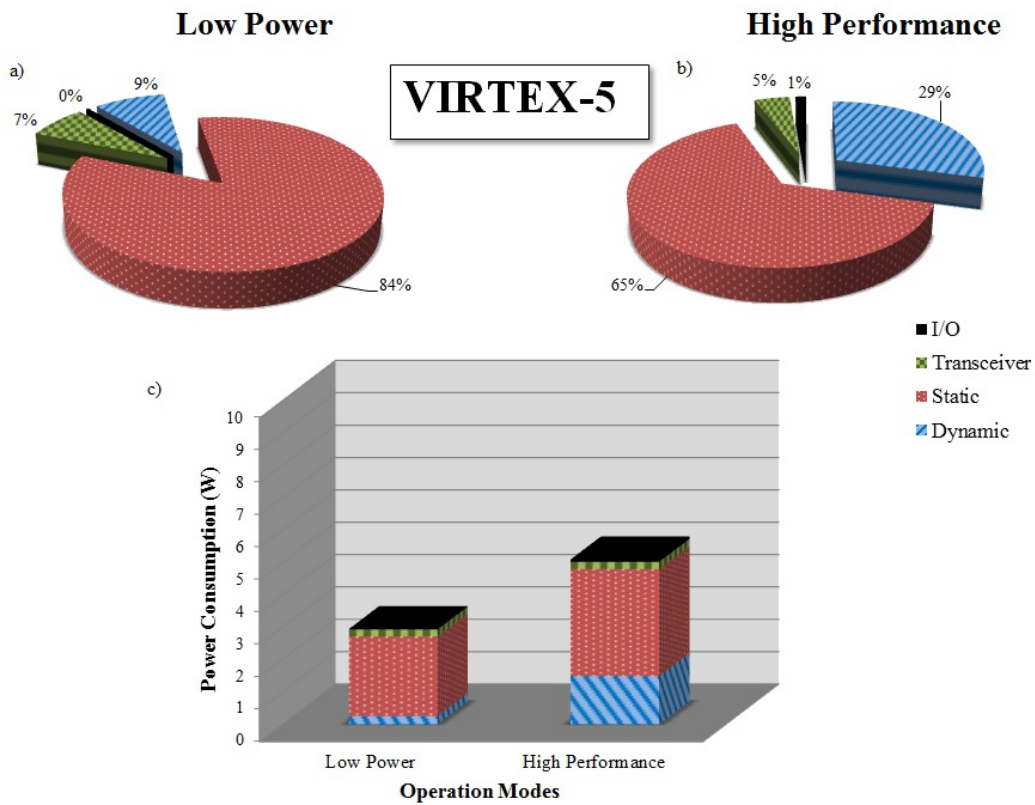


Figure 6. Total Power Usage in Xilinx® Virtex-5 Hardware Apparatus

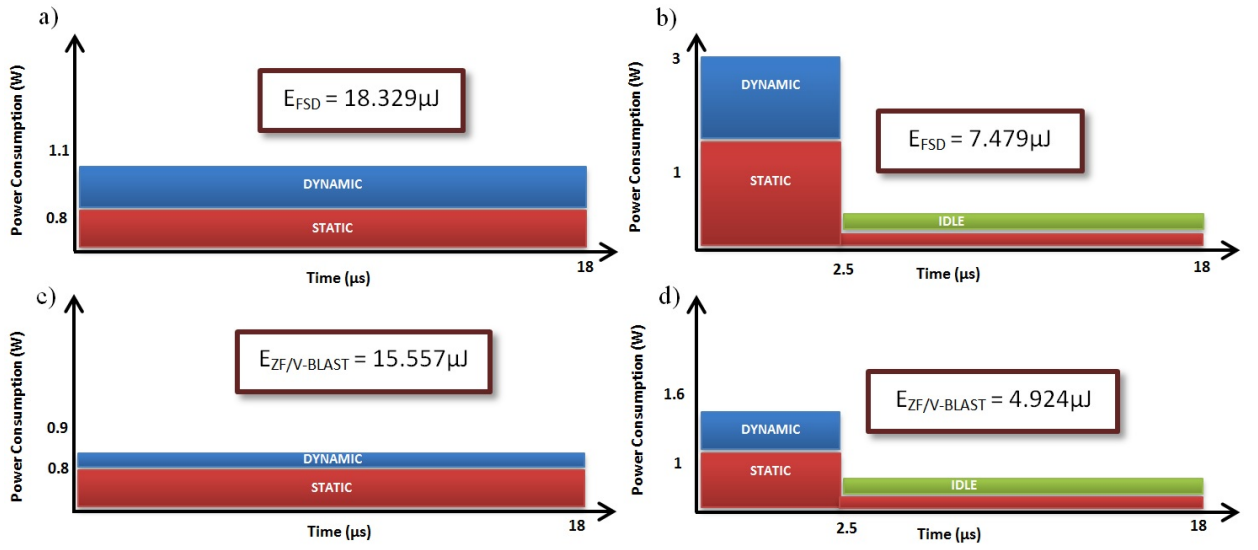


Figure 7. MIMO Detection FSD (a) and (b) in comparison with V-BLAST/ZF (c) and (d) for Low Power Mode and High Performance Mode respectively

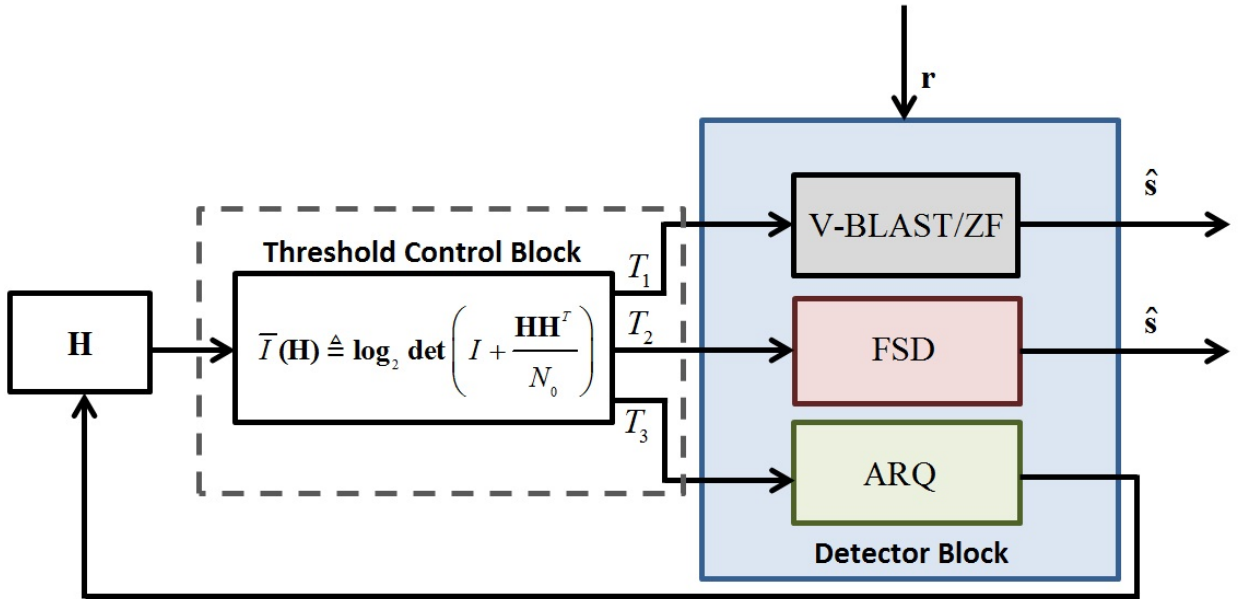


Figure 8. Simple Adaptive Algorithm Implementation Model

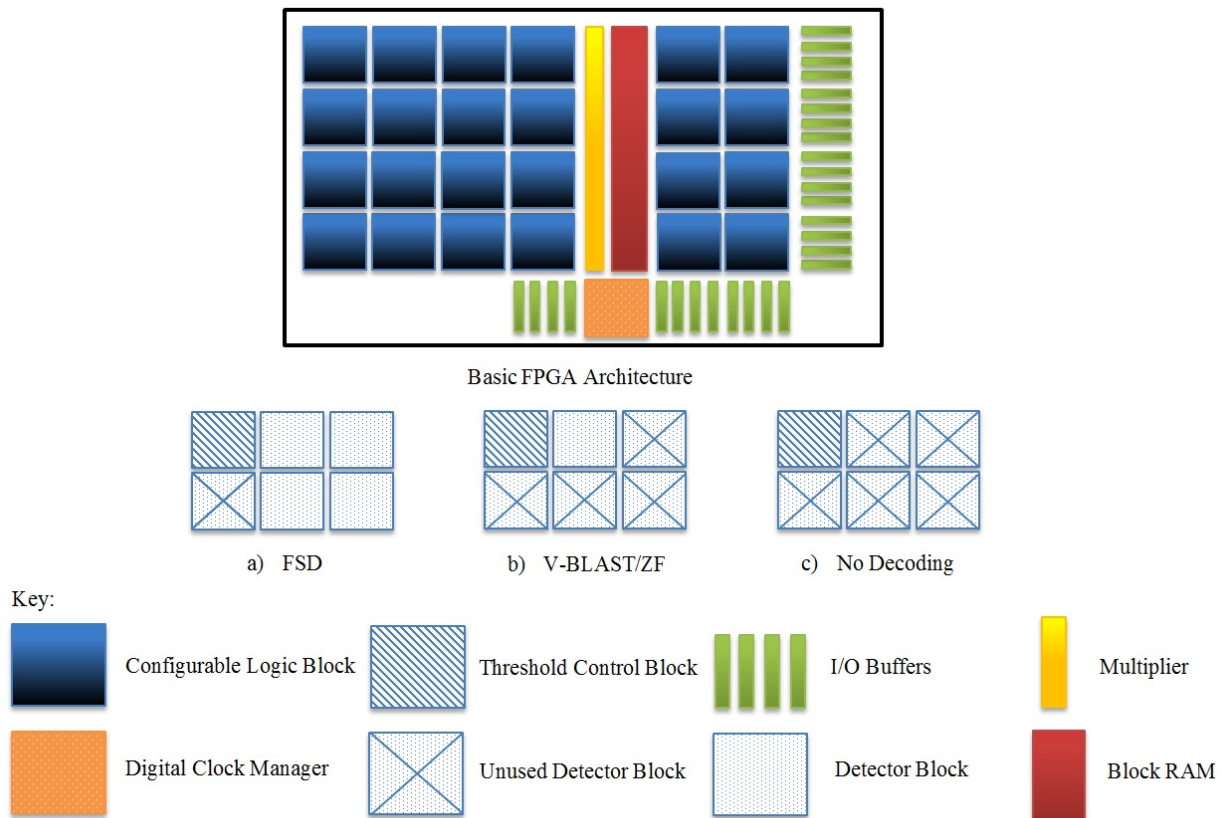


Figure 9. Total Resource Allocation of Adaptive Algorithm on a Basic FPGA Architecture

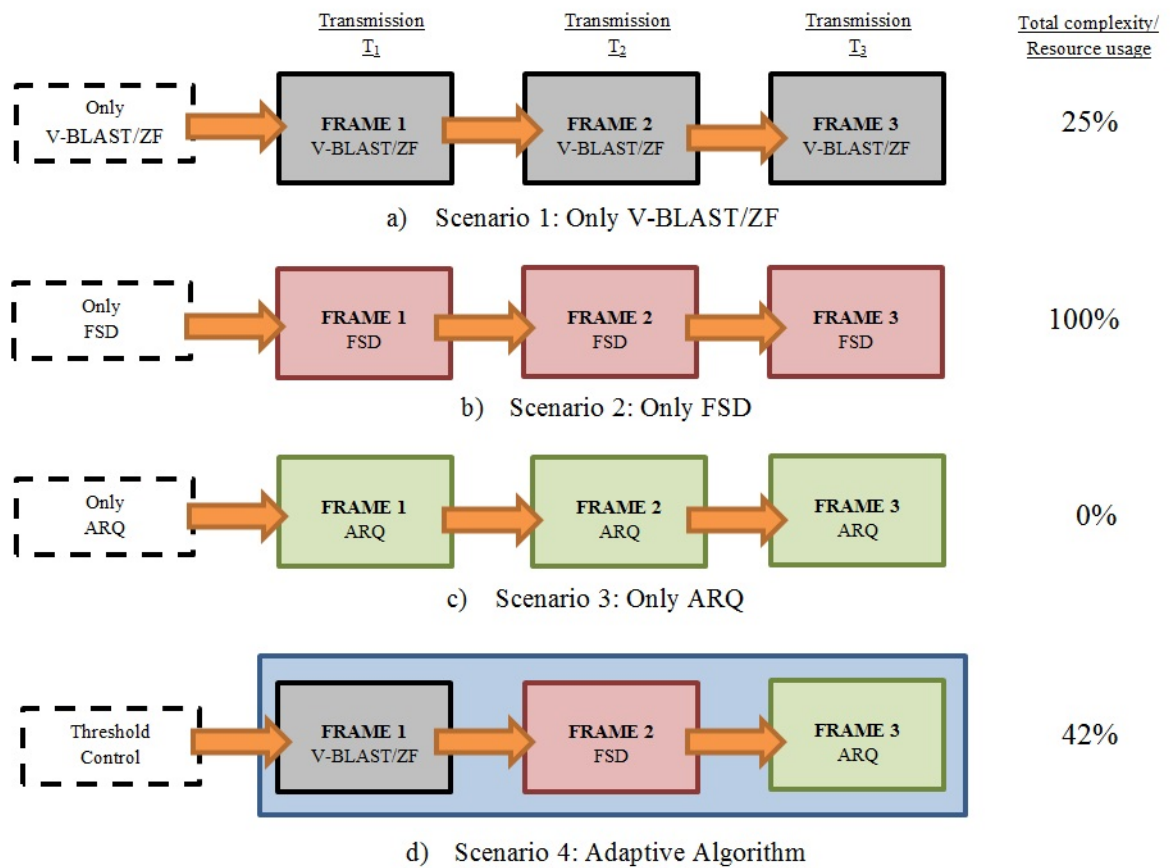


Figure 10. Basic Overview of the Inner Workings of the Adaptive Algorithm

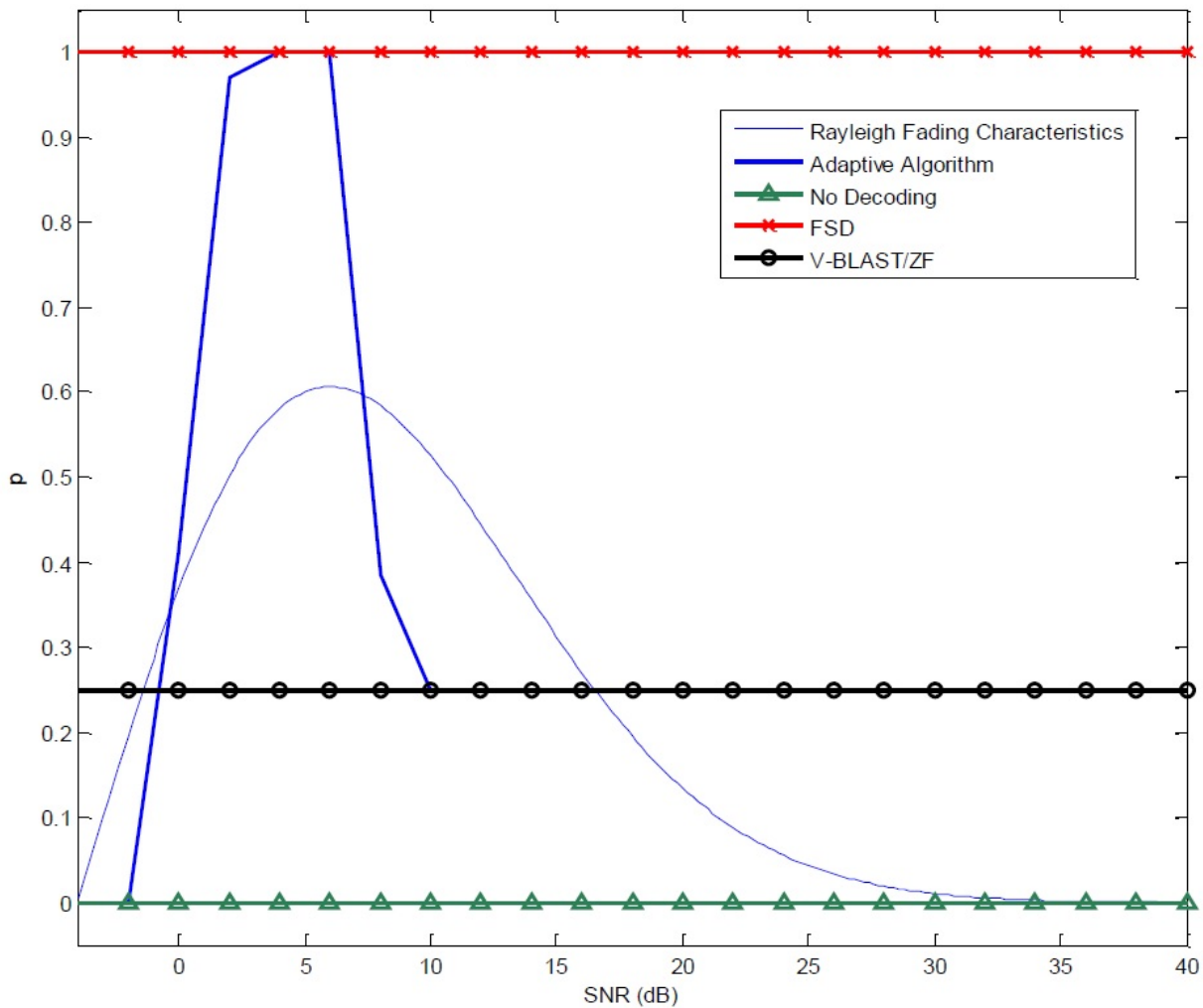


Figure 11. Behaviors of Different Detection Algorithms in a Rayleigh Fading Channel

Table 3. Virtex-5 Resource Utilization of Adaptive Algorithm

Logic Resource Utilization	Used	Available	Utilization
Slice Registers	13,683	149,760	9%
Flip Flops	4688	37,440	12%
4-Input LUTs	12,161	149,760	8%
DSP48E	132	1,056	12%
Memory (RAM)	28	516	5%

Virtex 5: XC5VLX330TFF1738

MIMO setup 4x4

Modulation Scheme 16-QAM

Bit Frame Size 1024 bits

Operation Mode Parameters	Low Power	High Performance
Core Voltage	0.95V	1.05V
Clock Frequency	60MHz	400MHz
Max Throughput	240Mbps	1200Mbps

Table 4. Experiment Parameters of Adaptive Algorithm